

Aryan, Homayon, Bortnik, Jacob, Kent Tobiska, W., Mehta, Piyush, Siddalingappa, Rashmi ORCID logoORCID: https://orcid.org/0000-0001-9786-8436 and Hogan, Benjamin (2025) Cross Correlation Between Plasmaspheric Hiss Waves and Enhanced Radiation Levels at Aviation Altitudes. Space Weather, 23 (2). e2024SW004184.

Downloaded from: https://ray.yorksj.ac.uk/id/eprint/12868/

The version presented here may differ from the published version or version of record. If you intend to cite from the work you are advised to consult the publisher's version: https://doi.org/10.1029/2024SW004184

Research at York St John (RaY) is an institutional repository. It supports the principles of open access by making the research outputs of the University available in digital form. Copyright of the items stored in RaY reside with the authors and/or other copyright owners. Users may access full text items free of charge, and may download a copy for private study or non-commercial research. For further reuse terms, see licence terms governing individual outputs. Institutional Repositories Policy Statement

# RaY

Research at the University of York St John
For more information please contact RaY at ray@yorksj.ac.uk



# Space Weather®

# <del>-</del>

#### RESEARCH ARTICLE

10.1029/2024SW004184

#### **Special Collection:**

Impact of Space Weather Events on Transportation System

#### **Key Points:**

- We study the correlation between plasmaspheric Hiss waves and enhanced radiation aviation altitude
- Strong indication that plasmaspheric hiss is the cause of the radiation enhancements at aviation altitudes
- Enhanced radiation levels are correlated with plasmaspheric hiss waves within ±1 L and 2 hr MLT

#### Correspondence to:

H. Aryan, aryan.homayon@gmail.com

#### Citation:

Aryan, H., Bortnik, J., Tobiska, W. K., Mehta, P., Siddalingappa, R., & Hogan, B. (2025). Cross correlation between plasmaspheric hiss waves and enhanced radiation levels at aviation altitudes. *Space Weather*, 23, e2024SW004184. https://doi.org/10.1029/2024SW004184

Received 24 SEP 2024 Accepted 18 JAN 2025

#### **Author Contributions:**

Conceptualization: Homayon Aryan
Data curation: W. Kent Tobiska
Investigation: Homayon Aryan
Methodology: Homayon Aryan
Software: Homayon Aryan
Supervision: Jacob Bortnik,
W. Kent Tobiska
Validation: Homayon Aryan
Visualization: Homayon Aryan
Writing – original draft:
Homayon Aryan
Writing – review & editing:
Homayon Aryan

© 2025. The Author(s).

This is an open access article under the terms of the Creative Commons

Attribution-NonCommercial-NoDerivs

License, which permits use and distribution in any medium, provided the original work is properly cited, the use is non-commercial and no modifications or adaptations are made.

# **Cross Correlation Between Plasmaspheric Hiss Waves and Enhanced Radiation Levels at Aviation Altitudes**

Homayon Aryan<sup>1</sup>, Jacob Bortnik<sup>1</sup>, W. Kent Tobiska<sup>2</sup>, Piyush Mehta<sup>3</sup>, Rashmi Siddalingappa<sup>3,4</sup>, and Benjamin Hogan<sup>2</sup>

<sup>1</sup>University of California Los Angeles, Atmospheric and Oceanic Sciences, Los Angeles, CA, USA, <sup>2</sup>Space Weather Division, Space Environment Technologies, Pacific Palisades, CA, USA, <sup>3</sup>West Virginia University, Mechanical and Aerospace Engineering, Morgantown, WV, USA, <sup>4</sup>Department of Computer Science, Christ University, Bangalore, Karnataka, India

**Abstract** Enhanced radiation in the Earth's atmosphere can pose serious hazards to pilots, aircraft passengers, and commercial space travelers. Recent results have shown, statistically, that there is a strong correlation between dose rates observed by Automated Radiation Measurements for Aerospace Safety (ARMAS) instruments at aviation altitudes (>9 km) and plasmaspheric hiss wave power measured by NASA's Van Allen Probes within the inner magnetosphere. Plasmaspheric hiss waves play a very important role in removing energetic electrons from the Earth's radiation belts by precipitating them into the upper atmosphere. These relativistic electrons generally drift eastwards along closed magnetic drift shells. In this study, we use magnetic conjunction events between ARMAS and the Van Allen Probes to analyze the causality between plasmaspheric hiss waves and enhanced radiation observed at aviation altitude. We specifically study how the size of the conjunction window and a shift in L and MLT of the conjunction window affect the correlation between dose rates and plasmaspheric hiss wave power. This is to determine if the observed enhanced radiation at aviation altitude is indeed caused by the plasmaspheric hiss waves in the inner magnetosphere. The results show that the enhanced radiation levels are only correlated with plasmaspheric hiss waves within conjunction windows of  $-1 \le L \le 1$  and  $0 \le MLT \le 2$ . The correlation between dose rate and hiss wave power increases slightly if ARMAS is shifted approximately 1 hr in MLT to the east of the Van Allen Probes, consistent with the drift trajectory of the electrons precipitating into the atmosphere.

Plain Language Summary Enhanced radiation in the Earth's atmosphere can pose serious hazards to pilots, aircraft passengers, and commercial space travelers. Recent results have shown, statistically, that there is a strong correlation between dose rates observed by Automated Radiation Measurements for Aerospace Safety (ARMAS) instruments at aviation altitudes (>9 km) and plasmaspheric hiss wave power measured by NASA's Van Allen Probes within the inner magnetosphere. Plasmaspheric hiss waves play a very important role in removing energetic electrons from the Earth's radiation belts by precipitating them into the upper atmosphere. These relativistic electrons generally drift eastwards along closed magnetic drift shells. In this study, we use magnetic conjunction events between ARMAS and the Van Allen Probes to determine if the observed enhanced radiation at aviation altitude is indeed caused by the plasmaspheric hiss waves. The correlation between dose rate and plasmaspheric hiss wave power increases slightly if ARMAS is shifted approximately 1 hr in MLT to the east of the Van Allen Probes, consistent with the drift trajectory of the electrons precipitating into the atmosphere. This is a strong indication that plasmaspheric hiss is the cause of the radiation enhancements measured by the ARMAS instruments at aviation altitudes.

#### 1. Introduction

The Earth's atmosphere is known to experience occasional periods of enhanced radiation that can pose a serious hazard to pilots, aircraft passengers, and commercial space travelers. Charged particles can enter the Earth's atmosphere over a wide range of magnetic latitudes and impact atmospheric molecules generating x-rays and gamma-rays in the process (Dwyer et al., 2012). Exposure to cosmic radiation can cause adverse health effects to air travelers, such as, increasing the risk of fatal cancer (Knipp, 2017) or other adverse health effects that can limit careers of aircrew (Cannon et al., 2013). It can also lead to Single Event Effects (SEEs) (Dyer et al., 2018; Normand, 1996; O'Bryan et al., 2009; Zheng et al., 2019).

ARYAN ET AL. 1 of 15

10.1029/2024SW004184



# **Space Weather**

The two major sources of radiation hazards are historically known to be the galactic cosmic rays (GCRs) and solar energetic particles (SEPs) (Reames, 2013; Vlahos et al., 2019). The SEPs originate from flaring events that are related to solar coronal mass ejections (CMEs) or from interplanetary magnetic field (IMF) shocks (Desai & Giacalone, 2016; Gopalswamy et al., 2004; Reames, 2013). The GCR's, on the other hand, are produced in high-energy explosive events outside the solar system and can be modulated slowly by the IMF (Blandford & Eichler, 1987). Some studies have used the Automated Radiation Measurements for Aerospace Safety (ARMAS) measurements at aviation altitudes (>9 km) to show that there is a third source of radiation, that may be linked to the relativistic electrons that are precipitated from the Van Allen radiation belts (Tobiska et al., 2018), possibly by electromagnetic ion cyclotron (EMIC) waves (Tobiska et al., 2022).

However, recently Aryan et al. (2023) demonstrated that the third source of radiation is actually related to precipitation of radiation belt electrons due to plasmaspheric hiss waves in the inner equatorial magnetosphere. Aryan et al. (2023) used conjunction events between ARMAS and NASA's Van Allen Probes to study the correlation between enhanced radiation levels at aviation altitudes (>9 km) and various plasma waves within the inner magnetosphere, including EMIC waves, Chorus waves, plasmaspheric hiss waves and high frequency waves. In the latter study, the conjunctions between ARMAS and the Van Allen Probes were confined to within 1 L (L-shell) and 1 h MLT. The results demonstrated strong statistical correlation between enhanced radiation levels observed by ARMAS at aviation altitudes (>9 km) and plasmaspheric hiss waves measured by the Van Allen Probes in the inner equatorial magnetosphere.

Plasmaspheric hiss waves play a very important role in removing energetic electrons from the Earth's radiation belts by precipitating them into the upper atmosphere. Through cyclotron resonant interactions, plasmaspheric hiss waves can pitch-angle scatter electrons with energies ranging from tens of keV up to several MeV (Horne & Thorne, 1998; Li et al., 2007; Ma et al., 2016; Ni et al., 2014; Ripoll et al., 2016, 2019, 2020a, 2020b). It is known that as well as spiraling and bouncing, the relativistic electrons also slowly drift eastwards along closed magnetic drift shells (Li et al., 2021; Ripoll et al., 2019, 2020a, 2020b; Roederer, 1967; Roederer & Zhang, 2014). Therefore, if the observed enhanced radiation at aviation altitude is indeed caused by the plasmaspheric hiss waves in the inner magnetosphere, then a shift in the magnetic conjunction window between ARMAS at aviation altitude and the Van Allen Probes in the inner magnetosphere would play a very important role in defining the relationship between dose rate and plasmaspheric hiss wave power reported by Aryan et al. (2023). In addition, the size of the conjunction window can also play a crucial role in defining the correlation between the observed dose rate at aviation altitudes and plasmaspheric hiss waves. For example, narrower conjunction windows may result in fewer events that are more closely related to one another but may also result in greater uncertainty due to fewer conjunction events in each smaller conjunction window. On the other hand, a wider conjunction window may deteriorate the correlation between enhanced radiation and plasmaspheric hiss wave power due to the fact that plasmaspheric hiss waves have a limited spatial extent and therefore some events within the same wider conjunction window may not be entirely related to one another.

In this study, we use magnetic conjunction events between ARMAS and the Van Allen Probes to analyze dependencies of the cross correlation between plasmaspheric hiss waves and enhanced radiation observed at aviation altitude. This is to determine if the observed enhanced radiation at aviation altitude is indeed caused by the plasmaspheric hiss waves in the inner magnetosphere. To achieve this, we first apply a shifts in MLT and L, respectively, to the conjunction windows (defined by L and MLT, please refer to the data and methodology section for further details) between ARMAS and the Van Allen Probes (i.e., shifting ARMAS in the MLT and L directions relative to the Van Allen Probes) and then examine how the size of the conjunction windows affects the correlation between enhanced radiation at aviation altitude and plasmaspheric hiss waves in the inner equatorial magnetosphere.

Section 2 provides a description of the data and methodology. In Section 3 and 4 we show how the size of the conjunction window and a shift in the conjunction window in MLT and L, respectively, affect the correlation between dose rates observed at aviation altitude by ARMAS and plasmaspheric hiss wave power observed by the Van Allen probes. Finally, the discussion and conclusions are provided in Section 5.

# 2. Data and Methodology

The radiation data in this study are measured by ARMAS instruments that are flown at aviation altitudes (>9 km) on commercial aircraft and various agency-sponsored flights, such as, the NASA Armstrong Flight Research

ARYAN ET AL. 2 of 15

Center (AFRC), the National Science Foundation (NSF), the National Center for Atmospheric Research (NCAR), the National Oceanic and Atmospheric Administration (NOAA), Gulfstream 5 (G-5), and commercial aircraft, and the Federal Aviation Administration (FAA) William J. Hughes Technical Center (WJHTC) Bombardier Global 5000 (BG5) (Tobiska et al., 2016, 2018, 2022). The ARMAS instruments operate in an automated radiation collection mode that provides continuous data for an entire flight in the form of 10-s measured absorbed dose and derived effective dose rates. The environment absorbed dose is measured in silicon (Si) on the aircraft. The data is then sent to the ground via an Iridium satellite link or aircraft WiFi through real-time data streaming. The data is then processed to Level 4 effective dose rates for location and time (Tobiska et al., 2016, 2018, 2022). A Teledyne micro dosimeter uDOS001 (uDOS), a microprocessor, a GPS chip, an Iridium transceiver or a Bluetooth transmitter, and other associated electronics are used to make the measurements. Extensive ground beam line testing have shown that the uDOS chip used is sensitive to heavy ions (Fe+), electrons, protons, neutrons, alphas, and  $\gamma$ -rays, especially above 1 MeV (Tobiska et al., 2016). The ARMAS database includes >1,000 flights from ground to above 500 km altitude providing >1,000,000 10-s measured absorbed dose and derived effective dose rates. The background dose rate, including GCR's and SEP's, are estimated NASA Langley Research Center (LaRC) Nowcast of Atmospheric Ionizing Radiation for Aviation Safety (NAIRAS) model (Mertens et al., 2013).

The wave data used in this study were measured by the two identical Van Allen Probes that studied the Van Allen radiation belts between 2012 and 2019. These satellites operated in a 10° inclination orbit with an apogee of approximately 5.8 RE and a perigee of 1.1 RE geocentric (Mauk et al., 2013). The wave data was measured by the Electric and Magnetic Field Instrument Suite and Integrated Science (EMFISIS) wave instruments onboard each probe (Kletzing et al., 2013). The Waveform Receiver was used to measure the wave power spectral density (PSD) between 10 Hz and 12 kHz (Kletzing et al., 2013; Wygant et al., 2013). The high-frequency receiver (HFR) was used to measure the electric spectral intensity between 10 and 400 kHz. A triaxial fluxgate magnetometer and a triaxial search coil magnetometer were used to measure the background magnetic fields the high frequency wave magnetic field fluctuations respectively (Kletzing et al., 2013), including continuous waveform burst mode with selected ~6 s snapshots. Plasmaspheric hiss waves are right-hand polarized electromagnetic whistler-mode waves (Bortnik et al., 2008, 2009; Thorne et al., 1973) that occur naturally inside the plasmasphere and dayside plasmaspheric plumes where the plasma density is high (Chan & Holzer, 1976; Hayakawa et al., 1986; Parrot & Lefeuvre, 1986). They are observed as a steady, incoherent noise band (Falkowski et al., 2017; Tsurutani et al., 2015, 2018) in the approximate frequency range of 100 Hz < f < 2 kHz (Meredith et al., 2004). Plasmaspheric hiss waves play an important role in the dynamics of the radiation belts. They are responsible for the continuous scattering of the inner radiation belt electrons into the atmospheric loss cone. It is also known that plasmaspheric hiss waves are responsible for the decay of energetic electrons in the outer radiation belt during relatively quiet geomagnetic conditions (Lyons & Thorne, 1973; Summers et al., 2007) that happens as a result of resonant pitch angle scattering of energetic electrons (Lyons et al., 1972). Plasmaspheric hiss waves are also crucial in the formation of the slot region between the inner and outer radiation belts (Albert, 1999; Lyons et al., 1972; Lyons & Thorne, 1973; Ripoll et al., 2015). For this study, we use the comprehensive wave data measured by the EMFISIS instruments onboard the two Van Allen Probes for the entire mission. The 3D magnetic field waveform survey data are used to calculate 1-min averaged wave PSD over the frequency range 100 Hz < f < 2 kHz for plasmaspheric hiss (Aryan et al., 2016, 2023; Meredith et al., 2004, 2007; Thorne et al., 1973). Note:  $\Delta D$  is the difference between the measured dose by ARMAS and the background dose estimated by NAIRAS model.

Figure 1 shows a close conjunction event between ARMAS and Van Allen Probe B on 28 December 2015. The lower panel shows a clear signature of plasmaspheric hiss waves observed by Van Allen Probe B on the dayside around MLT  $\approx$ 14hr and L  $\approx$ 3, whilst the upper panel shows that the ARMAS instruments measure dose rates (red bars) that are above the background level (blue line) at around 10 km altitude, MLT  $\approx$ 13 hr and L  $\approx$ 2. During this close conjunction the ARMAS instrument measures dose rates that increase and correlate well with the intensification of plasmaspheric hiss waves observed by Van Allen Probe B within the inner equatorial magnetosphere. This suggests that the enhanced radiation is linked to plasmaspheric hiss waves as reported by Aryan et al. (2023).

In this study, we use almost 7 years of ARMAS real-time radiation measurements at aviation altitudes (>9 km) and plasma wave data observed by NASA's Van Allen Probes in the inner magnetosphere (between 2013–2019). We identified >1,000 conjunction events between ARMAS and Van Allen Probes within a conjunction window

ARYAN ET AL. 3 of 15

15427390, 2025, 2, Downloaded from https://agupubs.onlinelibrary.wiley.com/doi/10.1029/2024SW004184 by NICE, National

Institute for Health and Care Excellence, Wiley Online Library on [04/11/2025]. See

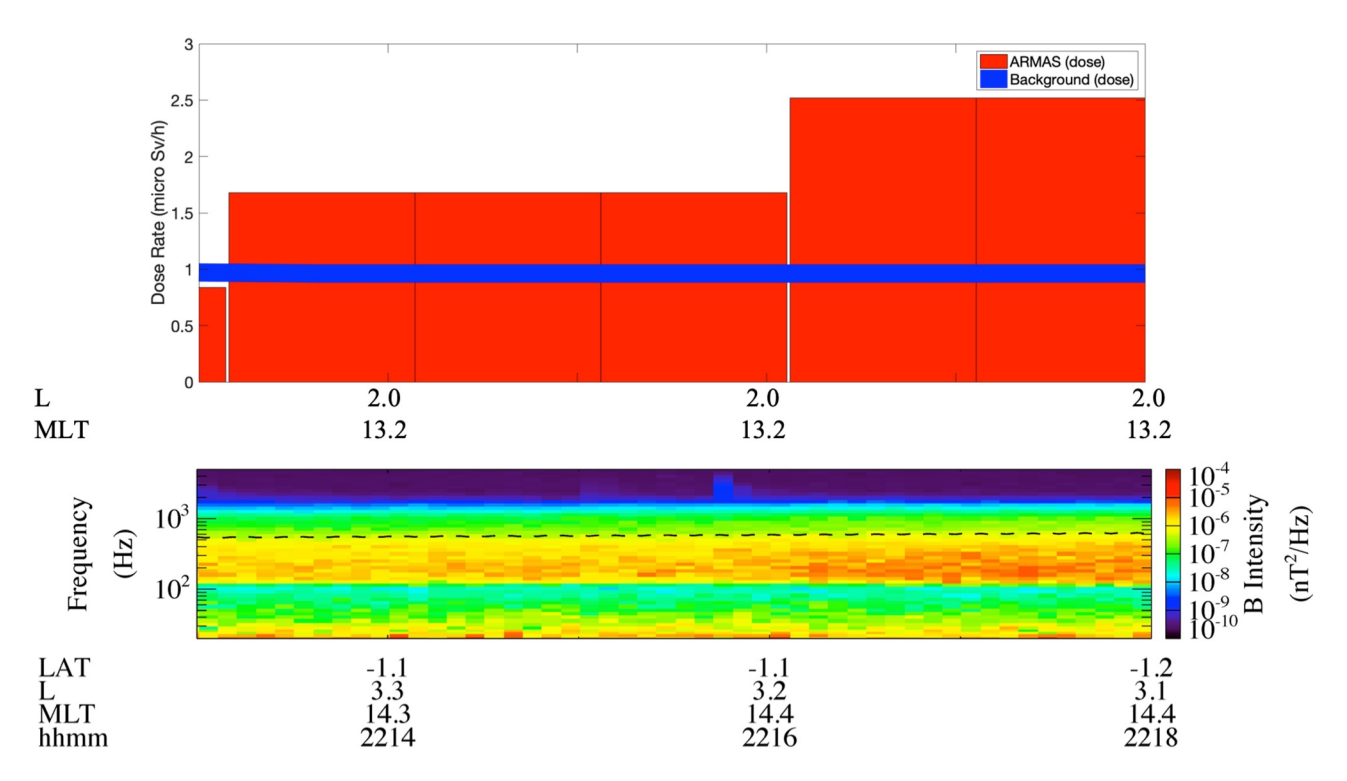


**Figure 1.** A conjunction event between ARMAS and Van Allen Probe B on 28 December 2015. The top panel shows the background dose rate (blue line) and the observed dose rate (red bars) measured by ARMAS at around 10 km altitude. The lower panel shows plasmaspheric hiss waves observed by Van Allen Probe B in the inner equatorial magnetosphere.

of  $\Delta L < 1$  RE and  $\Delta MLT < 1$  h. We use these conjunction events to study in detail the dependencies of the cross correlation between plasmaspheric hiss waves and enhanced radiation observed at aviation altitude.

Figure 2 shows the correlation between the dose rates observed by ARMAS at aviation altitudes and the plasmaspheric hiss wave power observed by the Van Allen Probes in the inner magnetosphere. The results show a strong correlation between dose rates and plasmaspheric hiss wave power as reported by Aryan et al. (2023), with a correlation coefficient r = 0.73, while the red line represents the line of best fit.

Aryan et al. (2023) investigated the correlation between dose rates and various wave modes that could be linked to the enhanced radiation observed at aviation altitudes, including electromagnetic ion cyclotron (EMIC) waves, chorus waves, and high-frequency waves. However, Aryan et al. (2023) concluded that dose rates were only correlated with plasmaspheric hiss wave power. Aryan et al. (2023) did not explore the correlation between dose rates and lightning-generated whistlers because terrestrial gamma ray flashes (TGFs) are not considered a credible source of this radiation for several reasons: (a) While TGFs from lighting have been documented (Pallu et al., 2023), they occur almost exclusively in the lower troposphere where the optical depth for photon absorption is quite high. In fact, the Pallu et al. (2023) study indicates that 200 m is the range of effective dose up to 1 Sv centered around the source, with the dose falling off dramatically the further away the sensor is from the source. Of the hundreds of thousands of aircraft flights in a 2-year period, Pallu et al. (2023) indicates that less than one aircraft will be hit by a TGF. (b) Of the 1,000+ tropospheric flights by ARMAS, zero flights have flown close to thunderstorms. The commercial, corporate, and agency flights that have hosted ARMAS all take great precautions to avoid thunderstorm areas. (c) The duration of the excess radiation seen by ARMAS lasts for tens of minutes to 2 hours while the aircraft is flying at a rate of 600 km/hr. TGFs, on the other hand, last for less than 1 s. There is no known lighting source that is continuous for tens of minutes to hours across several hundred km of distance. (d) The integration time for ARMAS when used on aircraft is at the minimum 10-s and those integration periods are processed on the ground to 1-min data records. A TGF is <1 s and even if there were one close TGF example out of a thousand flights, that is, at the 200 m and 1 Sv category, that signal would be lost in the integration of the remaining 59 s at GCR level dose rates. In other words, we simply would not be able to detect TGFs using the current ARMAS technology. (e) Lightning-generated whistler wave intensity is about 10 times smaller than hiss

ARYAN ET AL. 4 of 15

and Care Excellence, Wiley Online Library on [04/11/2025]. See

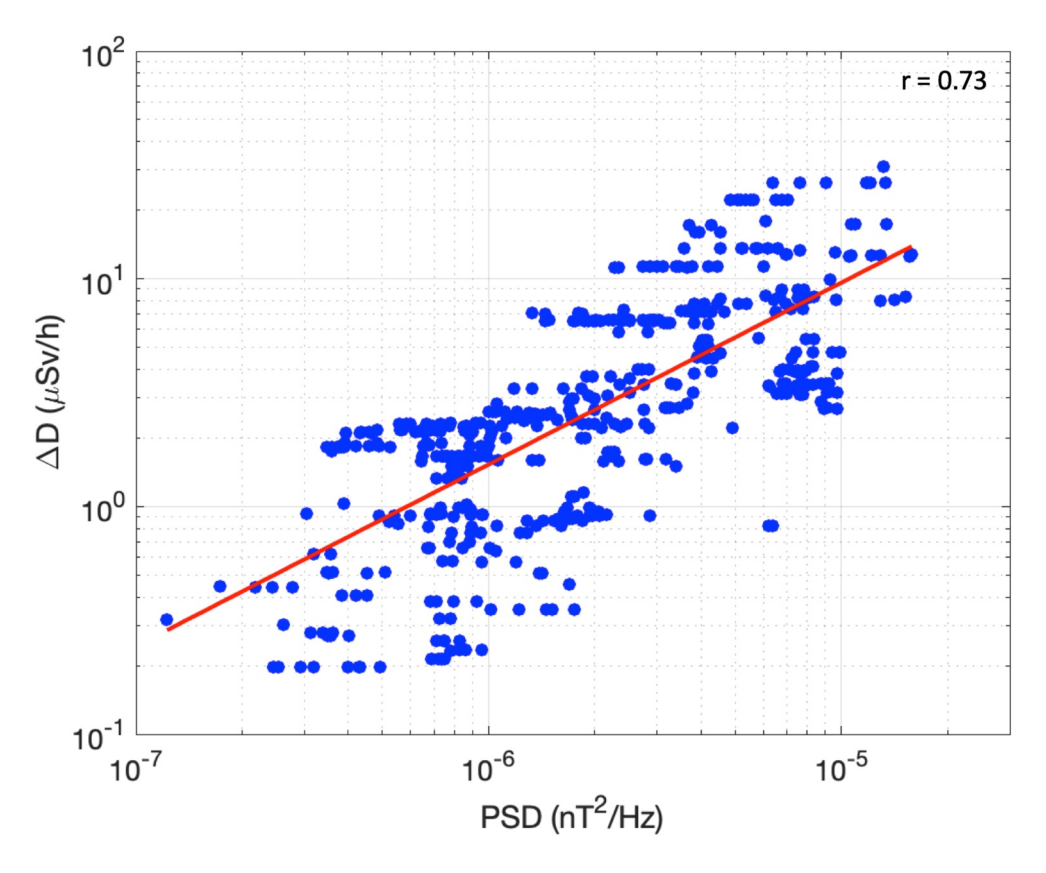


Figure 2. The relationship between the observed dose rate ( $\Delta D$ ) at aviation altitudes (>9 km) and plasmaspheric hiss wave power (power spectral density) in the inner equatorial magnetosphere. The red line represent the line of best fit and the correlation coefficient is given in the top right corner.

intensity as measured during CRRES (Meredith et al., 2007; NP et al., 2009) and Van Allen Probes (Green et al., 2020; Ripoll et al., 2020b, 2021) missions, which makes their effects in terms of electron precipitations 100 times weaker than the one produced by hiss waves.

Despite the reasons outlined above, we have examined the correlation between dose rates and lightning-generated whistlers wave power for the sake of completeness. The correlation between the 2–11 kHz frequency range, which corresponds to lightning-generated whistlers, and the dose rates observed by ARMAS is shown in Figure 3. As seen, the correlation coefficient is 0.2, indicating no significant relationship between the two.

There are approximately 700 data samples where the Van Allen Probes detected plasmaspheric hiss waves while ARMAS simultaneously measured enhanced radiation (i.e., radiation levels higher than the background). Each data point represents a 1-min average of plasmaspheric hiss intensities and corresponding dose rates. The geographical distribution of these ARMAS events are shown in Figure 4, with most events occurring over North America. Additionally, the global distribution of these events are presented in Figure 5, split into four MLT sectors.

The events are fairly well distributed in L-shell values, ranging from approximately 1.8–4.2 L. However, the events are not evenly spread across the MLT sectors, with a notably higher concentration in the post-noon sector (12:00–18:00 MLT), which is when plasmaspheric hiss waves are more likely to be observed (Aryan et al., 2021). Conversely, fewer events were recorded in the dawn sector (00:00–06:00 MLT). Despite this uneven distribution across MLT sectors, the correlation coefficient between dose rates and plasmaspheric hiss wave power remains relatively high across all MLT sectors.

It is also worth nothing that the majority of conjunction events occur around the aviation altitude (9–13 km), therefore the correlation coefficients presented in this study are unlikely to be affected significantly by altitude. To further investigate the potential impact of altitude on the observed correlation, we divided the data into two

ARYAN ET AL. 5 of 15

15427390, 2025, 2, Downloaded from https://agupubs.onlinelibrary.wiley.com/doi/10.1029/2024SW004184 by NICE, National Institute for Health and Care Excellence, Wiley Online Library on [0411/2025]. See the Term

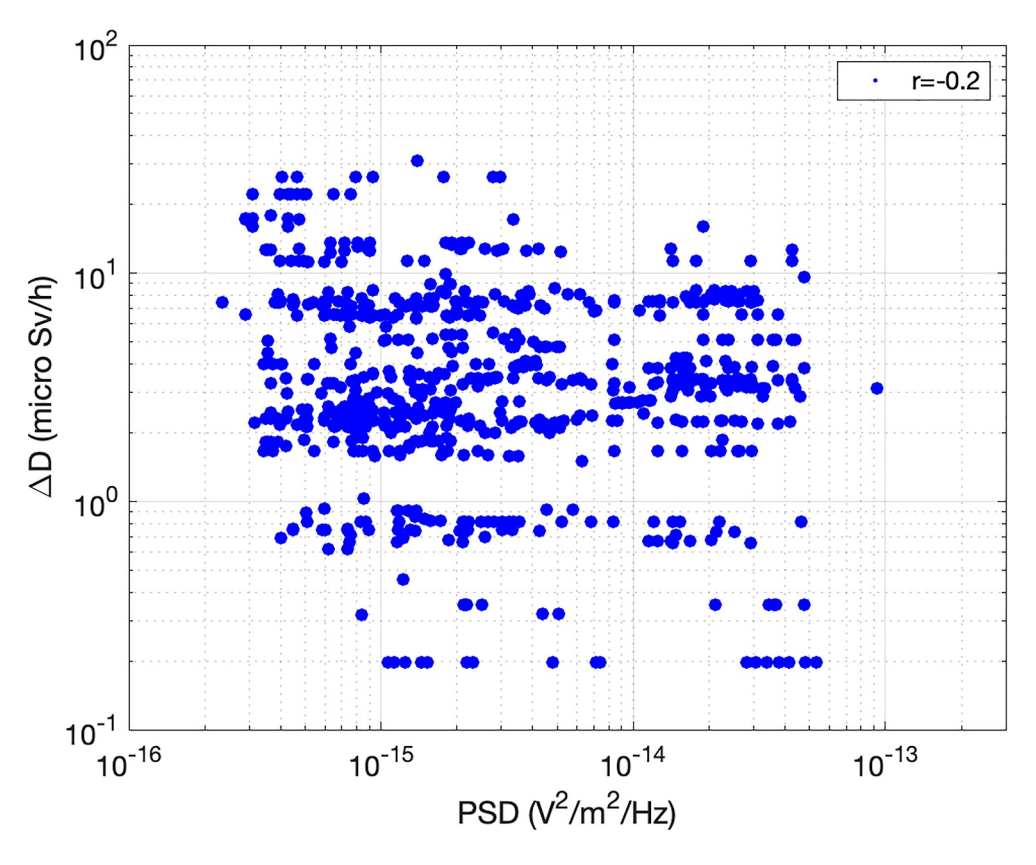


Figure 3. The relationship between the observed dose rate ( $\Delta D$ ) at aviation altitudes (>9 km) and lightning-generated whistler wave power (power spectral density) in the inner equatorial magnetosphere.

altitude bins: One for altitudes below 12 km and another for altitudes above 12 km. The correlation between plasmaspheric hiss wave power and dose rate was calculated separately for each of these altitude bins. The results, shown in Figure 6, reveal that the correlation coefficients for both altitude ranges are very similar, indicating that the relationship between hiss wave power and dose rates remains consistent across these two altitude ranges.

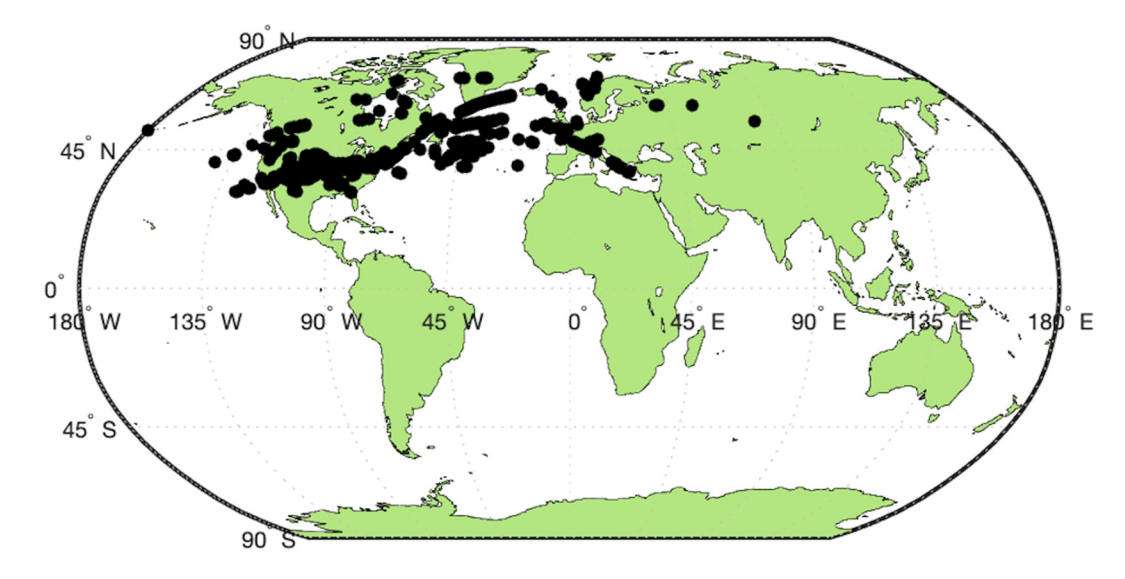


Figure 4. Geographical distribution of the ARMAS events.

ARYAN ET AL. 6 of 15

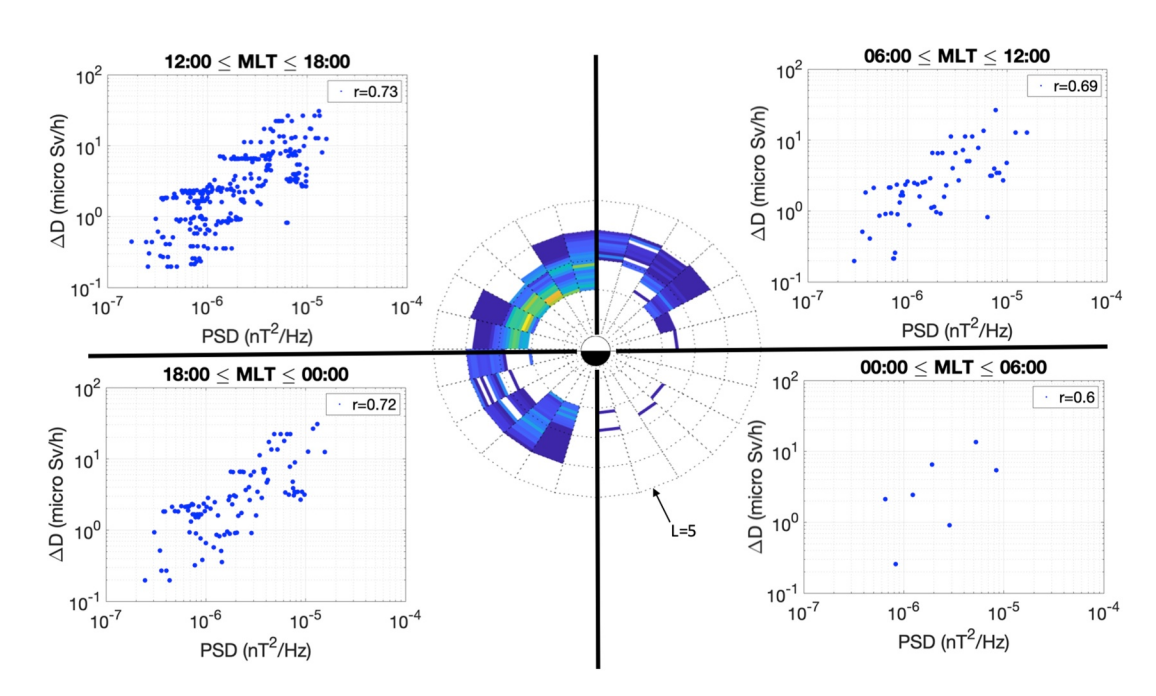


Figure 5. Global distribution of the ARMAS events.

For the low-altitude bin (altitudes <12 km), the correlation coefficient was found to be 0.71, with a standard error of  $\pm 0.16$ . For the high-altitude bin (altitudes >12 km), the correlation coefficient was similarly 0.74 with a standard error of  $\pm 0.17$ . Given the minimal difference in the correlation coefficients and the standard errors between the two altitude ranges, it is reasonable to conclude that altitude does not significantly affect the correlation between plasmaspheric hiss wave power and the observed dose rates. This suggests that the relationship between hiss wave power and radiation exposure is robust across the typical range of aviation altitudes.

To investigate if the observed enhanced radiation at aviation altitude is indeed caused by the plasmaspheric hiss waves in the inner magnetosphere then both the size of the conjunction window and a shift in the conjunction window will play crucial roles as described in the introduction section. To determine this, we first analyze the effect of changing the correlation window in L and MLT respectively on the correlation coefficients between plasmaspheric hiss waves power and enhanced radiation observed at aviation altitude. We then examine how the size of the conjunction window (i.e., the bin size) contributes to correlation coefficients between plasmaspheric hiss waves power and enhanced radiation.

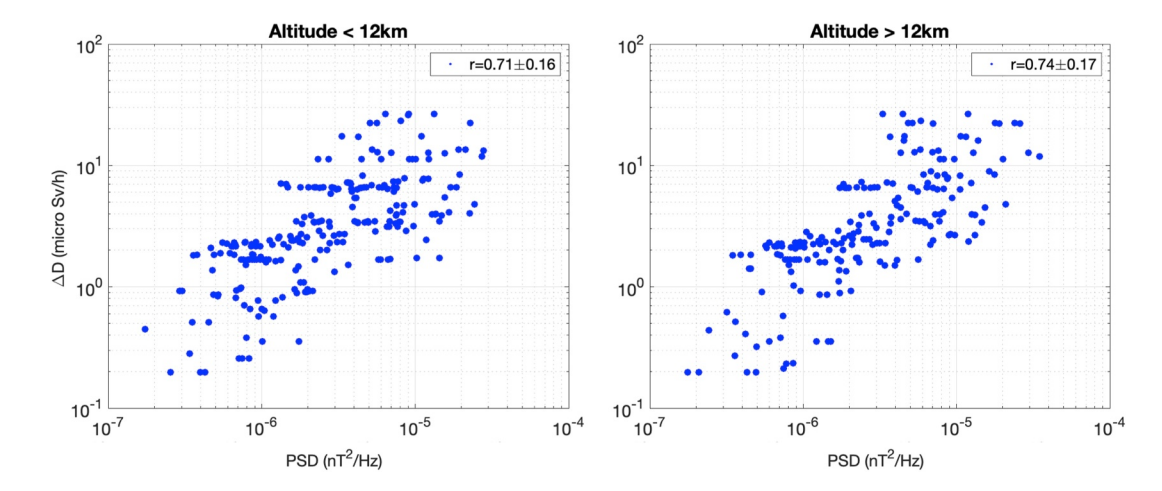


Figure 6. The relationship between the observed dose rate ( $\Delta$ D) at aviation altitudes (>9 km) and plasmaspheric hiss wave power (power spectral density) for (left) low and (right) high altitude flights.

ARYAN ET AL. 7 of 15

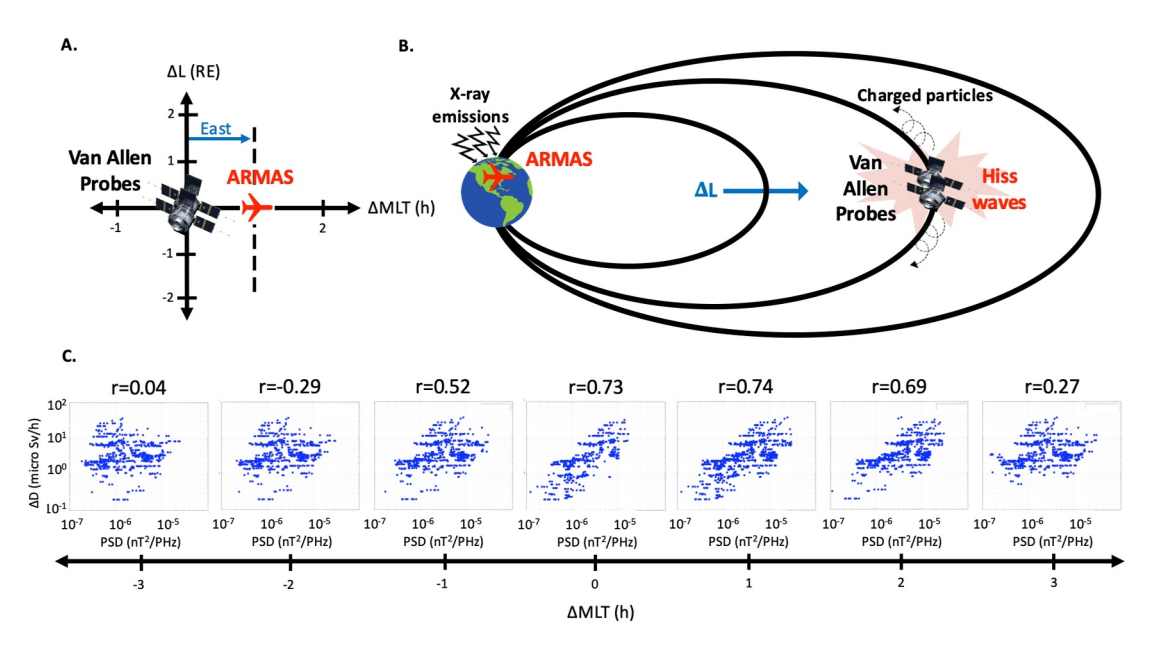


Figure 7. Panel A illustrates the conjunction window geometry with 1 h MLT shift for ARMAS relative to the Van Allen Probes. Panel B shows a schematic of the Van Allen Probes observing plasmaspheric hiss waves in the inner equatorial magnetosphere while in magnetic conjunction with ARMAS instrument at aviation altitudes. Panel C shows the variation of the correlation coefficient for different MLT shifts  $(-3 \le \Delta MLT \le 3)$  in the conjunction windows of ARMAS relative to the Van Allen Probes.

## 3. Effects of Changing Conjunction Window in Magnetic Local Time

The relativistic electrons slowly drift eastwards (Roederer, 1967) along closed magnetic drift shells as they are precipitated from the radiation belts into the upper atmosphere through cyclotron resonant interactions with plasmaspheric hiss waves. Here we apply various MLT shifts to the conjunction windows between ARMAS and the Van Allen Probes (i.e., we shift ARMAS in the MLT and L directions relative to the Van Allen Probes) to examine how it will influence the correlation between enhanced radiation levels and plasmaspheric hiss waves presented in Figure 2.

Figure 7a illustrates the conjunction window geometry with 1 h MLT shift for ARMAS relative to the Van Allen Probes (i.e., a positive  $\Delta$ MLT indicates an eastward shift of ARMAS relative to the Van Allen Probes and vice versa). Figure 7b provides a schematic of the Van Allen Probes observing plasmaspheric hiss waves in the inner equatorial magnetosphere while in magnetic conjunction with the ARMAS instrument at aviation altitudes. Figure 7c shows the variation of the correlation coefficient for different MLT shifts ( $-3 \le \Delta$ MLT  $\le 3$ ) in the conjunction windows of ARMAS relative to the Van Allen Probes. The results show that the correlation coefficients change for different MLT shifts. This is explored further in Figure 7, which shows the correlation coefficient as a function of  $\Delta$ MLT with error bars (the vertical lines that represent the standard error (SE) and are calculated by dividing the standard deviation ( $\sigma$ ) by the square root of the total number of data (n): SE =  $\sigma/\sqrt{n}$  (Altman & Bland, 2005)) and hourly MLT shift in the conjunction windows of ARMAS relative to the Van Allen Probes.

For a  $\Delta$ MLT = 0 the ARMAS is in the same MLT as the Van Allen Probes (i.e., ARMAS and the Van Allen Probes are in direct magnetic conjunction), and the correlation coefficient is r = 0.73 as shown in Figure 2. However, when the ARMAS is shifted by 1 h MLT to the east of the Van Allen Probes (i.e.,  $\Delta$ MLT = 1) the correlation coefficient remains high and even slightly higher (r = 0.74), which is an indication that enhanced radiation observed at aviation altitude is closely associated with the intensity of plasmaspheric hiss waves at the inner equatorial magnetosphere. This is consistent with the drift path of relativistic electrons from the Van Allen radiation belts, as they are drifting eastward. The correlation coefficient decreases to r = 0.69 when the ARMAS is shifted by 2 h MLT to the east of the Van Allen Probes, which is still relatively high and an indication that the ARMAS and the Van Allen Probes conjunction window is still within the spatial extent of plasmaspheric hiss waves and the drift path of relativistic electrons. However, the correlation coefficients are much smaller and very

ARYAN ET AL. 8 of 15

and Care Excellence, Wiley Online Library on [04/11/2025]. See the

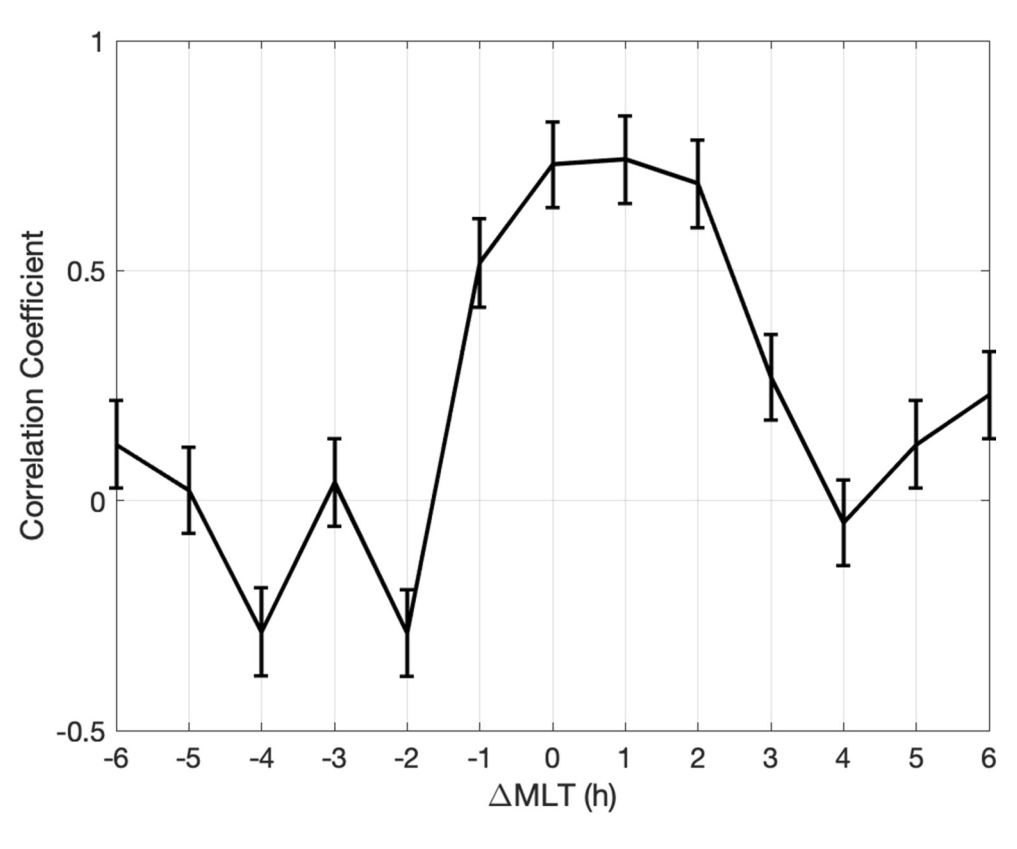


Figure 8. The correlation coefficient as a function of  $\Delta$ MLT with error bars (vertical lines) and hourly MLT shift in the conjunction windows of ARMAS at aviation altitudes (>9 km) relative to the Van Allen Probes in the inner magnetosphere.

random when the conjunction window is shifted beyond 2 h MLT since the relativistic electrons would have already precipitated to the dense upper atmosphere by this point. Also the correlation coefficients are much smaller and very random when the ARMAS is shifted westwards of the Van Allen Probes (i.e., for  $\Delta$ MLT <0) which indicates a weak relationship between the dose rates and plasmaspheric hiss waves. The correlation coefficient for a 1 h westward MLT shift is r=0.59 in comparison to the correlation coefficient for 1 h eastward MLT shift, which emphasizes that the precipitating relativistic electrons from the Van Allen radiation belts due to plasmaspheric hiss wave scattering are directly related to the enhanced radiation levels observed at the aviation altitudes (>9 km).

The size of the conjunction window can also play a very important role in defining the correlation between the observed dose rate at aviation altitudes (>9 km) and plasmaspheric hiss waves in the inner equatorial magnetosphere. The results discussed in Figure 8 are based on a conjunction window size of 1 h MLT (i.e., each bin contains events that occur within a specific 1 h MLT conjunction window). Here we reduce the conjunction window to 0.5 hr MLT to determine how the relationship between dose rate and plasmaspheric hiss wave power is affected.

Figure 9 shows the correlation coefficient as a function of  $\Delta$ MLT with error bars (vertical lines) and 0.5 hr MLT shift in the conjunction windows of ARMAS at aviation altitudes (>9 km) relative to the Van Allen Probes in the inner magnetosphere. Overall, the results show that the correlation coefficients are similar to correlation coefficients observed in Figure 8 with the highest correlation coefficient values observed for  $\Delta$ MLT between 0 and 2 h MLT. However, the peak correlation coefficient is r = 0.76 (observed for  $\Delta$ MLT = 1.5 MLT) which is slighty larger than the peak correlation coefficient r = 0.74 observed for  $\Delta$ MLT = 1 MLT with conjunction window size of 1 h MLT as of Figure 8. This demonstrates that narrower conjunction windows slightly improves the correlation coefficient between dose rate and plasmaspheric hiss wave power because the events within the narrower conjunction windows are more likely to be related to one another. Thus, the high correlation found demonstrate the enhanced radiation observed at aviation altitude is caused by the plasmaspheric hiss waves in the inner magnetosphere during these events. Though, narrower conjunction windows lead to greater uncertainty due to

ARYAN ET AL. 9 of 15

com/doi/10.1029/2024SW004184 by NICE, National Institute for Health and Care Excellence, Wiley Online Library on [04/11/2025]. See the

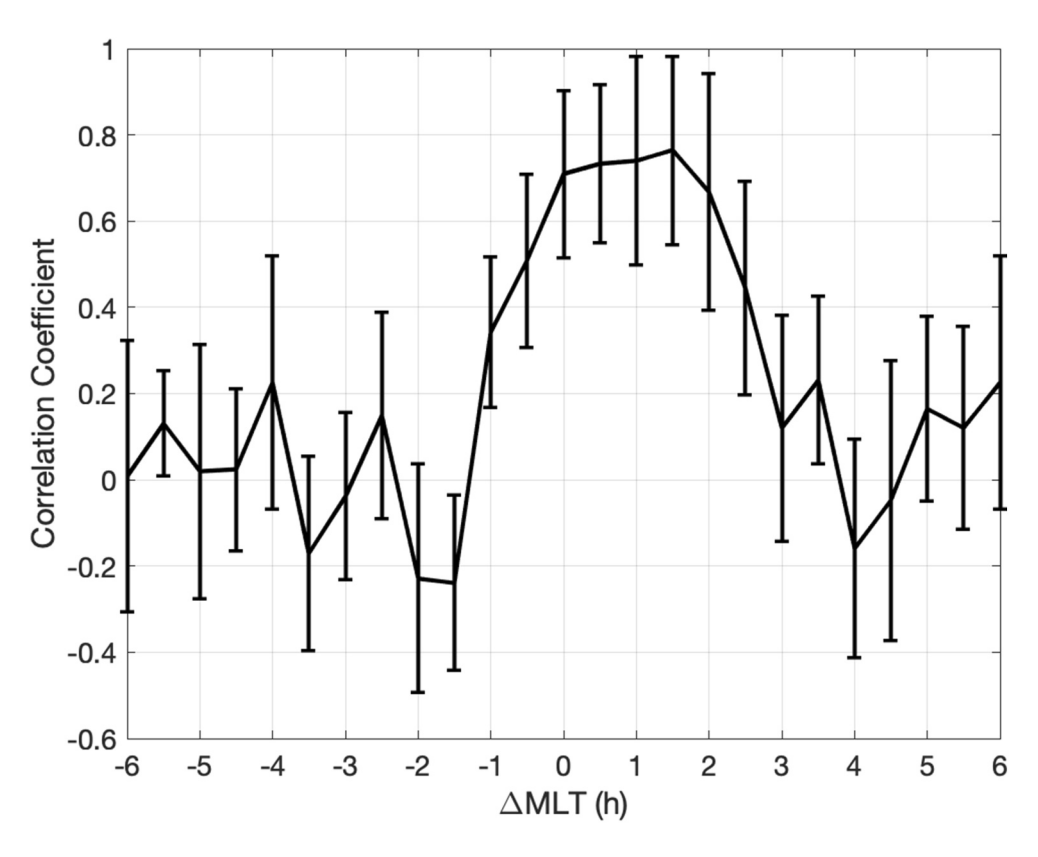


Figure 9. The correlation coefficient as a function of  $\Delta$ MLT with error bars (vertical lines) and 0.5 hr MLT shift in the conjunction windows of ARMAS at aviation altitudes (>9 km) relative to the Van Allen Probes in the inner magnetosphere.

smaller number of samples (approximately halved) in each smaller conjunction window as demonstrated by the larger error bars in Figure 8.

## 4. Effects of Changing Conjunction Window in L-Shell

Another important analysis to check the dependencies of the cross correlation between plasmaspheric hiss waves and enhanced radiation observed at aviation altitude is to study how the relationship between dose rate and plasmaspheric hiss wave changes with various shifts in L-shell. If the observed enhanced radiation at aviation altitude is indeed caused by the plasmaspheric hiss waves in the inner magnetosphere, then a shift in the magnetic conjunction window between ARMAS at aviation altitude and the Van Allen Probes in the inner magnetosphere would play a very important role in defining the correlation between the two due to limited spatial extent of plasmaspheric hiss waves. Here we apply various shifts in the L direction to the conjunction windows between ARMAS and the Van Allen Probes (i.e., shifting ARMAS in the L directions relative to the Van Allen Probes) to examine how it will influence the correlation between enhanced radiation levels and plasmaspheric hiss waves presented in Figure 2.

Figure 10 shows the correlation coefficient as a function of  $\Delta L$  with error bars (vertical lines) and 1 L shift in the conjunction windows of ARMAS at aviation altitudes (>9 km) relative to the Van Allen Probes in the inner magnetosphere. For  $\Delta L = 0$  the ARMAS is in the same L-shell as the Van Allen Probes and the correlation coefficient is r = 0.73 (as shown in Figure 2), which is also the peak correlation coefficient value for any  $\Delta L$ . However, a shift in the conjunction window of ARMAS relative to the Van Allen Probes, in either L direction, results in a decrease in the correlation coefficient. For example, the correlation coefficient decreases to r = 0.68, r = 0.46, and r = -0.13 for  $\Delta L = 1$ ,  $\Delta L = 2$ , and  $\Delta L = 3$  respectively. The number of samples in each bin also decreases from ~700 samples for  $\Delta L = 0$  to ~300 samples for  $\Delta L = 3$  (a similar pattern is observed for negative  $\Delta L$  values). This shows that the further the shift in conjunction window of ARMAS relative to the Van Allen Probes in the L-shell (i.e., the larger the  $\Delta L$ ) the lower the correlation coefficients, which indicates that enhanced radiation observed by ARMAS at aviation altitudes becomes less dependent to plasmaspheric hiss wave

ARYAN ET AL. 10 of 15

doi/10.1029/2024SW004184 by NICE, National Institute for Health and Care Excellence, Wiley Online Library on [04/11/2025]. See

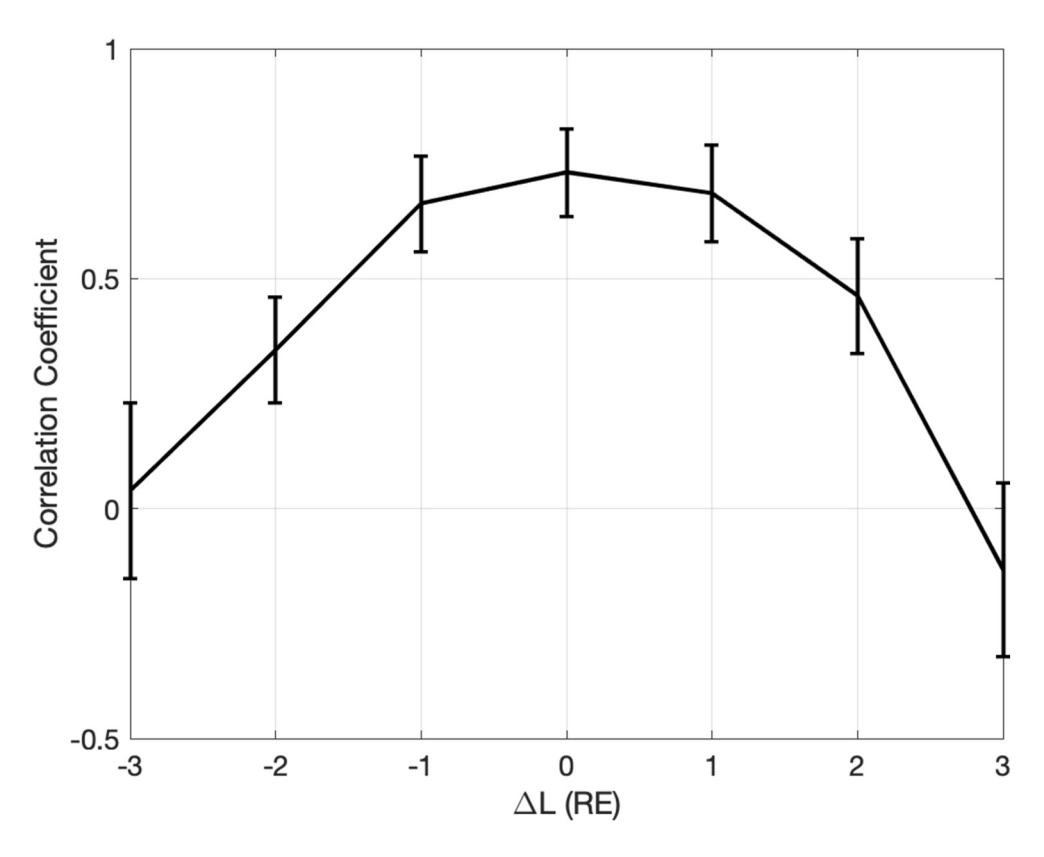


Figure 10. The correlation coefficient as a function of  $\Delta L$  with error bars (vertical lines) and 1 L shift in the conjunction windows of ARMAS at aviation altitudes (>9 km) relative to the Van Allen Probes in the inner magnetosphere.

observations by the Van Allen Probes. This is understandable as the further apart ARMAS and the Van Allen Probes are in L-shell the least likely they would be observing the same related event because plasmaspheric hiss waves have a limited spatial and temporal coherence (Zhang et al., 2021). In addition, it is worth noting that the results show that the error bars increase for larger  $\Delta L$  values. This is because for larger  $\Delta L$  values there are fewer samples and therefore greater uncertainty and error values.

The size of the conjunction window in L-shell can also play a very important role in defining the correlation between the observed dose rate at aviation altitudes and plasmaspheric hiss waves in the inner equatorial magnetosphere. The results discussed in Figure 7 are based on a conjunction window size of 1 L (i.e., each bin contains events that occur within a specific 1 L conjunction window). Here we examine how those results would change if the conjunction window is reduced to 0.5 L.

Figure 11 shows the correlation coefficient as a function of  $\Delta L$  with error bars (vertical lines) and 0.5 L shift in the conjunction windows of ARMAS at aviation altitudes relative to the Van Allen Probes in the inner magnetosphere. The peak correlation coefficient is r=0.78 observed for  $\Delta L=0$ , which is larger than the peak correlation coefficient r=0.73 observed for  $\Delta L=0$  with conjunction window size of 1 L as of Figure 10. However, the error bars are noticeably larger compared to Figure 10 which again indicates an increase in the uncertainty in the results due to lack of data in each smaller conjunction window. Similar to the results presented in Figure 8 for narrower MLT conjunction windows, the results here also demonstrate that narrower conjunction windows increase the correlation coefficient between dose rate and plasmaspheric hiss wave power because the events within the narrower conjunction windows are more likely to be related to one another, that is, the enhanced radiation observed at aviation altitude is caused by the plasmaspheric hiss waves in the inner magnetosphere during these events. Though, narrower conjunction windows lead to greater uncertainty due to smaller number of samples (e.g., less than 100 samples for  $\Delta L=\pm 3$ ) in each narrower conjunction window.

ARYAN ET AL.

15427390, 2025, 2, Downloaded from https://agupubs

i/10.1029/2024SW004184 by NICE, National Institute for Health and Care Excellence, Wiley Online Library on [04/11/2025]. See the

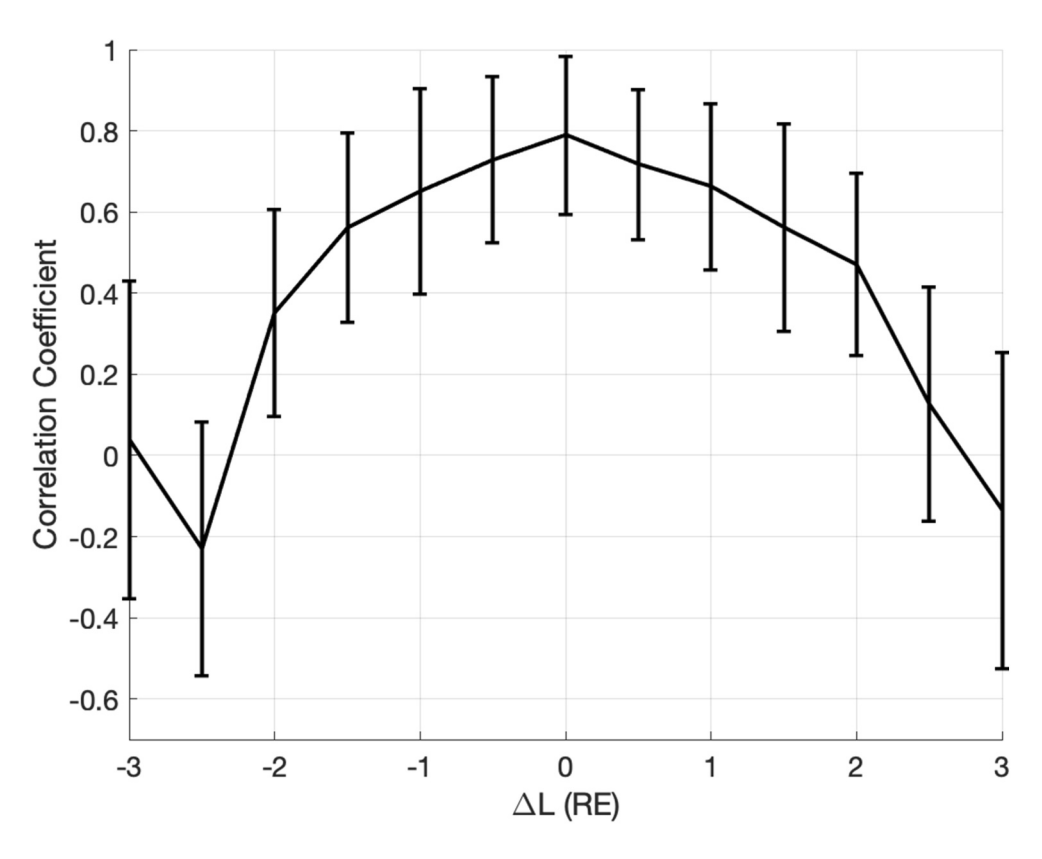


Figure 11. The correlation coefficient as a function of  $\Delta L$  with error bars (vertical lines) and 0.5 L shift in the conjunction windows of ARMAS at aviation altitudes (>9 km) relative to the Van Allen Probes in the inner magnetosphere.

### 5. Discussion and Conclusions

In this study, we used magnetic conjunction events between ARMAS and the Van Allen Probes to test the dependencies of the cross correlation between plasmaspheric hiss waves and enhanced radiation observed at aviation altitude. We used almost 7 years of ARMAS real-time radiation measurements taken at aviation altitudes (>9 km) and plasma wave data observed by NASA's Van Allen Probes in the inner magnetosphere (between 2013 – 2019). We identified >1,000 conjunctions between ARMAS and Van Allen Probes within a conjunction window of  $\Delta L < 1RE$  and  $\Delta MLT < 1h$ . We used these conjunctions to identify events where ARMAS observed enhanced radiation at aviation altitude while Van Allen probes observed plasmaspheric hiss waves in the inner magnetosphere. We then used the events to examine the influence of plasmaspheric hiss waves on enhanced radiation observed at aviation altitude. We specifically studied how the size of the conjunction window and a shift in the conjunction window in L and MLT affect the correlation between dose rates and plasmaspheric hiss wave power. The main goal of this study was to determine if the observed enhanced radiation at aviation altitude is indeed consistent with scattering by plasmaspheric hiss in the inner magnetosphere. To achieve that, we first applied shifts in MLT and L, respectively, to conjunction windows between ARMAS and the Van Allen Probes (i.e., shifting ARMAS in the MLT and L directions relative to the Van Allen Probes) and then examined how the size of the conjunction windows affects the correlation between enhanced radiation at aviation altitude and plasmaspheric hiss waves in the inner equatorial magnetosphere.

The results show that the enhanced radiation levels are only correlated with plasmaspheric hiss waves within conjunction windows of  $-1 \le L \le 1$  and  $0 \le MLT \le 2$  h. In addition, when ARMAS is shifted by 1 h MLT to the east of the Van Allen Probes (i.e.,  $\Delta$ MLT = 1) the correlation coefficient increased slightly from r = 0.73 to r = 0.74, which is consistent with the drift path of relativistic electrons from the Van Allen radiation belts, as they are drifted eastward. However, the correlation coefficients were much smaller and random when the conjunction window was shifted beyond 2 h MLT and when the ARMAS was shifted westwards of the Van Allen Probes (i.e., for  $\Delta$ MLT < 0) which indicated a weak relationship between the dose rates and plasmaspheric hiss waves. Also, a shift in the conjunction window of ARMAS relative to the Van Allen Probes, in either L direction, results in a

ARYAN ET AL. 12 of 15

decrease in the correlation coefficients. The largest correlation coefficient was observed when ARMAS was in the same L-shell as the Van Allen Probes (i.e.,  $\Delta L = 0$ ). These results are consistent with electron scattering through cyclotron resonant interactions with plasmaspheric hiss waves, and provide a strong indication that the enhanced radiation levels observed at the aviation altitudes are directly related to plasmaspheric hiss waves observed in the inner equatorial magnetosphere. In addition, the results also shows that the conjunction window size also plays an important role. For narrower conjunction, windows increase the correlation coefficients but lead to greater uncertainty due to a smaller number of events in each smaller conjunction window. Finally, the results show that the events are evenly distributed in L (between approximately 1.8–4.2 L), but more concentrated in the post-noon sector (between 12:00–18:00 MLT) where plasmaspheric hiss waves are likely to be observed. However, despite the uneven distribution of events in MLT, the correlation coefficient between the dose rates and plasmaspheric hiss wave power is relatively high for all MLT sectors.

Overall, the results provided here demonstrates that the enhanced radiation observed at the aviation altitude by ARMAS is most likely caused by the plasmaspheric hiss waves in the inner magnetosphere measured by the Van Allen probes. This could help us better understand the effect of plasmaspheric hiss waves on the energetic radiation belt electron precipitation, its spatial extent, and the relation to radiation experienced by commercial airline passengers, pilots, and space travelers.

## **Data Availability Statement**

The HFR and WFR data are freely available from the EMFISIS instrument (Kletzing et al., 2013; Wygant et al., 2013) website at the University of Iowa (https://emfisis.physics.uiowa.edu/). The geomagnetic index (AE) are freely available from NASA's GSFC online space physics data facility, OMNIWeb (https://omniweb.gsfc.nasa.gov). The ARMAS data is freely available from Space Environment Technologies ARMAS website at https://spacewx.com/radiation-decision-aids/. The ARMAS-RBSP conjunction list can be found at https://doi.org/10.5281/zenodo.14579779.

#### Acknowledgments

This study is supported by NASA's Living With Start (LWS) program (NASA/LWS-ARMAS: 443956-BR-23267).

#### References

- Albert, J. M. (1999). Analysis of quasi-linear diffusion coefficients. *Journal of Geophysical Research*, 104(A2), 2429–2441. https://doi.org/10.1029/1998JA900113
- Altman, D. G., & Bland, J. M. (2005). Standard deviations and standard errors. *BMJ*, 331(7521), 903. https://doi.org/10.1136/bmj.331.7521.903
  Aryan, H., Bortnik, J., Meredith, N. P., Horne, R. B., Sibeck, D. G., & Balikhin, M. A. (2021). Multi-parameter chorus and plasmaspheric hiss wave models. *Journal of Geophysical Research: Space Physics*, 126(1), e2020JA028403. https://doi.org/10.1029/2020JA028403
- Aryan, H., Bortnik, J., Tobiska, W. K., Mehta, P., & Siddalingappa, R. (2023). Enhanced radiation levels at aviation altitudes and their relationship to plasma waves in the inner magnetosphere. *Journal of Geophysical Research Space Weather*, 21(10). https://doi.org/10.1029/2023sw003477 Aryan, H., Sibeck, D., Balikhin, M., Agapitov, O., & Kletzing, C. (2016). Observation of chorus waves by the Van Allen Probes: Dependence on
- Aryan, H., Sibeck, D., Balikhin, M., Agapitov, O., & Kletzing, C. (2016). Observation of chorus waves by the Van Allen Probes: Dependence on solar wind parameters and scale size. *Journal of Geophysical Research (Space Physics)*, 121(8), 7608–7621. https://doi.org/10.1002/2016JA022775
- Blandford, R., & Eichler, D. (1987). Particle acceleration at astrophysical shocks: A theory of cosmic ray origin. *Physics Reports*, 154(1), 1–75. https://doi.org/10.1016/0370-1573(87)90134-7
- Bortnik, J., Li, W., Thorne, R. M., Angelopoulos, V., Cully, C., Bonnell, J., et al. (2009). An observation linking the origin of plasmaspheric hiss to discrete chorus emissions. *Science*, 324(5928), 775–778. https://doi.org/10.1126/science.1171273
- Bortnik, J., Thorne, R. M., & Meredith, N. P. (2008). The unexpected origin of plasmaspheric hiss from discrete chorus emissions. *Nature*, 452(7183), 62–66. https://doi.org/10.1038/nature06741
- Cannon, P., Angling, M., Barclay, L., Curry, C., Dyer, C., & Edwards, R. (2013). Extreme space weather: Impacts on engineered systems and infrastructure. Royal Academy of Engineering.
- Chan, K.-W., & Holzer, R. E. (1976). ELF hiss associated with plasma density enhancements in the outer magnetosphere. *Journal of Geophysical Research*, 81(13), 2267–2274. https://doi.org/10.1029/JA081i013p02267
- Desai, M., & Giacalone, J. (2016). Large gradual solar energetic particle events. Living Reviews in Solar Physics, 13(1), 3. https://doi.org/10.1007/s41116-016-0002-5
- Dwyer, J. R., Smith, D. M., & Cummer, S. A. (2012). High-energy atmospheric physics: Terrestrial gamma-ray flashes and related phenomena. Space Science Reviews, 173(1), 133–196. https://doi.org/10.1007/s11214-012-9894-0
- Dyer, C., Hands, A., Ryden, K., & Lei, F. (2018). Extreme atmospheric radiation environments and single event effects. *IEEE Transactions on Nuclear Science*, 65(1), 432–438. https://doi.org/10.1109/TNS.2017.2761258
- Falkowski, B. J., Tsurutani, B. T., Lakhina, G. S., & Pickett, J. S. (2017). Two sources of dayside intense, quasi-coherent plasmaspheric hiss: A new mechanism for the slot region? *Journal of Geophysical Research: Space Physics*, 122(2), 1643–1657. https://doi.org/10.1002/2016JA023289
- Gopalswamy, N., Yashiro, S., Krucker, S., Stenborg, G., & Howard, R. A. (2004). Intensity variation of large solar energetic particle events associated with coronal mass ejections. *Journal of Geophysical Research*, 109(A12). https://doi.org/10.1029/2004JA010602
- Green, A., Li, W., Ma, Q., Shen, X.-C., Bortnik, J., & Hospodarsky, G. B. (2020). Properties of lightning generated whistlers based on van Allen Probes observations and their global effects on radiation belt electron loss. *Geophysical Research Letters*, 47(17), e2020GL089584. https://doi.org/10.1029/2020GL089584

ARYAN ET AL. 13 of 15

15427390, 2025, 2, Downl

- Hayakawa, M., Ohmi, N., Parrot, M., & Lefeuvre, F. (1986). Direction finding of ELF hiss emissions in a detached plasma region of the magnetosphere. *Journal of Geophysical Research*, 91(A1), 135–142. https://doi.org/10.1029/JA091iA01p00135
- Horne, R. B., & Thorne, R. M. (1998). Potential waves for relativistic electron scattering and stochastic acceleration during magnetic storms. Geophysical Research Letters, 25(15), 3011–3014. https://doi.org/10.1029/98GL01002
- Kletzing, C. A., Kurth, W. S., Acuna, M., MacDowall, R. J., Torbert, R. B., Averkamp, T., et al. (2013). The electric and magnetic field instrument suite and integrated science (EMFISIS) on RBSP. Space Science Reviews, 179(1-4), 127-181. https://doi.org/10.1007/s11214-013-9993-6
- Knipp, D. J. (2017). Essential science for understanding risks from radiation for airline passengers and crews. Space Weather, 15(4), 549–552. https://doi.org/10.1002/2017SW001639
- Li, W., Shprits, Y. Y., & Thorne, R. M. (2007). Dynamic evolution of energetic outer zone electrons due to wave-particle interactions during storms. *Journal of Geophysical Research (Space Physics)*, 112(A11), 10220. https://doi.org/10.1029/2007JA012368
- Li, Z., Elkington, S., Hudson, M., Patel, M., Boyd, A., & Wygant, J. (2021). Modeling advective transport of radiation belt electrons. *Journal of Atmospheric and Solar-Terrestrial Physics*, 214, 105509. https://doi.org/10.1016/j.jastp.2020.105509
- Lyons, L. R., & Thorne, R. M. (1973). Equilibrium structure of radiation belt electrons. *Journal of Geophysical Research*, 78(13), 2142–2149. https://doi.org/10.1029/JA078i013p02142
- Lyons, L. R., Thorne, R. M., & Kennel, C. F. (1972). Pitch-angle diffusion of radiation belt electrons within the plasmasphere. *Journal of Geophysical Research*, 77(19), 3455–3474. https://doi.org/10.1029/JA077i019p03455
- Ma, Q., Li, W., Thorne, R. M., Nishimura, Y., Zhang, X.-J., Reeves, G. D., et al. (2016). Simulation of energy-dependent electron diffusion processes in the Earth's outer radiation belt. *Journal of Geophysical Research (Space Physics)*, 121(5), 4217–4231. https://doi.org/10.1002/ 2016JA022507
- Mauk, B. H., Fox, N. J., Kanekal, S. G., Kessel, R. L., Sibeck, D. G., & Ukhorskiy, A. (2013). Science objectives and rationale for the radiation belt storm probes mission. Space Science Reviews, 179(1-4), 3-27. https://doi.org/10.1007/s11214-012-9908-y
- Meredith, N. P., Horne, R. B., Glauert, S. A., & Anderson, R. R. (2007). Slot region electron loss timescales due to plasmaspheric hiss and lightning-generated whistlers. *Journal of Geophysical Research (Space Physics)*, 112(A8), A08214. https://doi.org/10.1029/2007JA012413
- Meredith, N. P., Horne, R. B., Thorne, R. M., Summers, D., & Anderson, R. R. (2004). Substorm dependence of plasmaspheric hiss. *Journal of Geophysical Research (Space Physics)*, 109(A6), 6209. https://doi.org/10.1029/2004JA010387
- Mertens, C. J., Meier, M. M., Brown, S., Norman, R. B., & Xu, X. (2013). Nairas aircraft radiation model development, dose climatology, and initial validation. Space Weather, 11(10), 603–635. https://doi.org/10.1002/swe.20100
- Ni, B., Li, W., Thorne, R. M., Bortnik, J., Ma, Q., Chen, L., et al. (2014). Resonant scattering of energetic electrons by unusual low-frequency hiss. Geophysical Research Letters, 41(6), 1854–1861. https://doi.org/10.1002/2014GL059389
- Normand, E. (1996). Single-event effects in avionics. *IEEE Transactions on Nuclear Science*, 43(2), 461–474. https://doi.org/10.1109/23.490893
  Np. M., Rb, H., Sa, G., Dn, B., Sg, K., & Jm, A. (2009). Relativistic electron loss timescales in the slot region. *Journal of Geophysical Research*.
- 114(A03222). https://doi.org/10.1029/2008JA013889
  O'Bryan, M. V., LaBel, K. A., Pellish, J. A., Buchner, S. P., Ladbury, R. L., Oldham, T. R., et al. (2009). Single event effects compendium of
- o Bryan, M. V., Labet, K. A., Penish, J. A., Buchner, S. P., Ladoury, K. L., Oldnam, T. R., et al. (2009). Single event effects compendium of candidate spacecraft electronics for nasa. In 2009 ieee radiation effects data workshop (pp. 15–24). https://doi.org/10.1109/REDW.2009. 5336321
- Pallu, M., Celestin, S., Trompier, F., & Klerlein, M. (2023). Radiation risk assessment associated with terrestrial gamma ray flashes for commercial flights. *Journal of Geophysical Research: Atmospheres*, 128(6), e2022JD037569. https://doi.org/10.1029/2022JD037569
- Parrot, M., & Lefeuvre, F. (1986). Statistical study of the propagation characteristics of ELF hiss observed on GEOS-1, inside and outside the plasmasphere. *Annales Geophysicae*, 4, 363–383.
- Reames, D. (2013). The two sources of solar energetic particles. Space Science Reviews, 175(1-4), 53-92. https://doi.org/10.1007/s11214-013-9958-9
- Ripoll, J.-F., Chen, Y., Fennell, J. F., & Friedel, R. H. W. (2015). On long decays of electrons in the vicinity of the slot region observed by heo3. *Journal of Geophysical Research: Space Physics*, 120(1), 460–478. https://doi.org/10.1002/2014JA020449
- Ripoll, J.-F., Claudepierre, S. G., Ukhorskiy, A. Y., Colpitts, C., Li, X., Fennell, J. F., & Crabtree, C. (2020a). Particle dynamics in the earth's radiation belts: Review of current research and open questions. *Journal of Geophysical Research: Space Physics*, 125(5), e2019JA026735. https://doi.org/10.1029/2019JA026735
- Ripoll, J.-F., Claudepierre, S. G., Ukhorskiy, A. Y., Colpitts, C., Li, X., Fennell, J. F., & Crabtree, C. (2020b). Particle dynamics in the earth's radiation belts: Review of current research and open questions. *Journal of Geophysical Research: Space Physics*, 125(5), e2019JA026735. https://doi.org/10.1029/2019JA026735
- Ripoll, J. F., Farges, T., Malaspina, D. M., Cunningham, G. S., Hospodarsky, G. B., Kletzing, C. A., & Wygant, J. R. (2021). Propagation and dispersion of lightning-generated whistlers measured from the Van Allen Probes. Frontiers in Physics, 9, 457. https://doi.org/10.3389/fphy. 2021.722355
- Ripoll, J.-F., Loridan, V., Denton, M. H., Cunningham, G., Reeves, G., Santolík, O., et al. (2019). Observations and Fokker-Planck simulations of the l-shell, energy, and pitch angle structure of earth's electron radiation belts during quiet times. *Journal of Geophysical Research: Space Physics*, 124(2), 1125–1142. https://doi.org/10.1029/2018JA026111
- Ripoll, J.-F., Reeves, G. D., Cunningham, G. S., Loridan, V., Denton, M., Santolík, O., et al. (2016). Reproducing the observed energy-dependent structure of earth's electron radiation belts during storm recovery with an event-specific diffusion model. *Geophysical Research Letters*, 43(11), 5616–5625. https://doi.org/10.1002/2016GL068869
- Roederer, J. G. (1967). On the adiabatic motion of energetic particles in a model magnetosphere. *Journal of Geophysical Research* (1896-1977), 72(3), 981–992. https://doi.org/10.1029/JZ072i003p00981
- Roederer, J. G., & Zhang, H. (2014). Dynamics of magnetically trapped particles. Springer. https://doi.org/10.1007/978-3-642-41530-2
- Summers, D., Ni, B., & Meredith, N. P. (2007). Timescales for radiation belt electron acceleration and loss due to resonant wave-particle interactions: 2. Evaluation for VLF chorus, ELF hiss, and electromagnetic ion cyclotron waves. *Journal of Geophysical Research (Space Physics)*, 112(A4), 4207. https://doi.org/10.1029/2006JA011993
- Thorne, R. M., Smith, E. J., Burton, R. K., & Holzer, R. E. (1973). Plasmaspheric hiss. *Journal of Geophysical Research*, 78(10), 1581–1596. https://doi.org/10.1029/JA078i010p01581
- Tobiska, W. K., Bouwer, D., Smart, D., Shea, M., Bailey, J., Didkovsky, L., et al. (2016). Global real-time dose measurements using the Automated Radiation Measurements for Aerospace Safety (ARMAS) System. Space Weather, 14(11), 1053–1080. https://doi.org/10.1002/
- Tobiska, W. K., Didkovsky, L., Judge, K., Weiman, S., Bouwer, D., Bailey, J., et al. (2018). Analytical representations for characterizing the global aviation radiation environment based on model and measurement databases. *Space Weather*, 16(10), 1523–1538. https://doi.org/10.1029/2018SW001843

ARYAN ET AL. 14 of 15

and Care Excellence, Wiley Online Library on [04/11/2025]. See the Terms

- Tobiska, W. K., Halford, A. J., & Morley, S. K. (2022). Increased radiation events discovered at commercial aviation altitudes. *Space Weather*. https://doi.org/10.48550/arXiv.2209.05599
- Tsurutani, B. T., Falkowski, B. J., Pickett, J. S., Santolik, O., & Lakhina, G. S. (2015). Plasmaspheric hiss properties: Observations from polar. Journal of Geophysical Research: Space Physics, 120(1), 414–431. https://doi.org/10.1002/2014JA020518
- Tsurutani, B. T., Park, S. A., Falkowski, B. J., Lakhina, G. S., Pickett, J. S., Bortnik, J., et al. (2018). Plasmaspheric hiss: Coherent and intense. Journal of Geophysical Research: Space Physics, 123(12), 10009–10029. https://doi.org/10.1029/2018JA025975
- Vlahos, L., Anastasiadis, A., Papaioannou, A., Kouloumvakos, A., & Isliker, H. (2019). Sources of solar energetic particles. *Philosophical Transactions of the Royal Society A: Mathematical, Physical & Engineering Sciences*, 377(2148), 20180095. https://doi.org/10.1098/rsta.2018. 0095
- Wygant, J. R., Bonnell, J. W., Goetz, K., Ergun, R. E., Mozer, F. S., Bale, S. D., et al. (2013). The electric field and waves instruments on the radiation belt storm probes mission. *Space Science Reviews*, 179(1–4), 183–220. https://doi.org/10.1007/s11214-013-0013-7
- Zheng, Y., Ganushkina, N. Y., Jiggens, P., Jun, I., Meier, M., Minow, J. I., et al. (2019). Space radiation and plasma effects on satellites and aviation: Quantities and metrics for tracking performance of space weather environment models. Space Weather, 17, 1384–1403. https://doi.org/10.1029/2018SW002042

ARYAN ET AL. 15 of 15